

## EDGE ARTICLE

View Article Online  
View Journal | View IssueCite this: *Chem. Sci.*, 2023, 14, 1485

All publication charges for this article have been paid for by the Royal Society of Chemistry

Received 16th November 2022  
Accepted 6th January 2023

DOI: 10.1039/d2sc06303d

rsc.li/chemical-science

# Three-component reductive conjugate addition/aldol tandem reaction enabled by nickel/photoredox dual catalysis†

Hongping Zhao<sup>a</sup> and Weiming Yuan <sup>abc</sup>

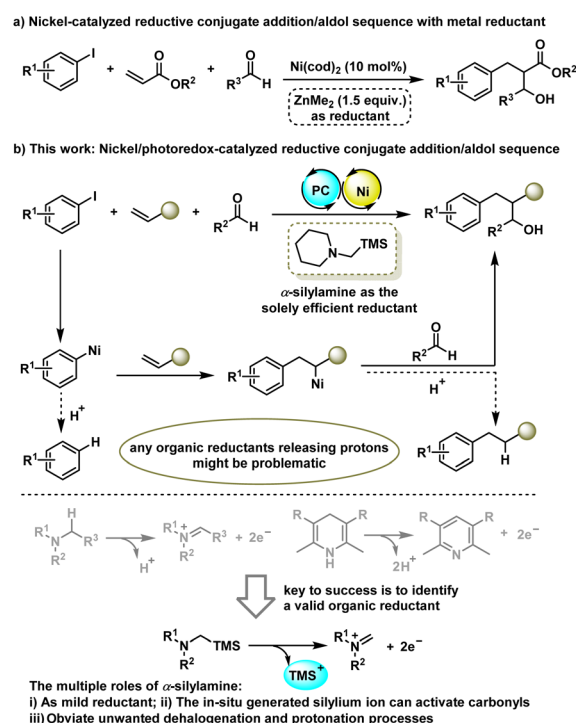
A three-component reductive cross-coupling of aryl halides, aldehydes, and alkenes by nickel/photoredox dual catalysis is disclosed. The key to success for this tandem transformation is to identify  $\alpha$ -silylamine as a unique organic reductant, which releases silylium ions instead of protons to prevent unwanted protonation processes, and meanwhile serves as Lewis acid to activate aldehydes *in situ*. This dual catalytic protocol completes a traditional conjugate addition/aldol sequence that eliminates the requirement of organometallic reagents and metal-based reductants, thus providing a mild synthetic route to highly valuable  $\beta$ -hydroxyl carbonyl compounds with contiguous 1,2-stereocenters.

## Introduction

Transition-metal-catalysed intermolecular three-component dicarbofunctionalization (DCF) of alkenes represents a powerful strategy to synthesize complex structures *via* simultaneously forging two vicinal carbon–carbon bonds in a single step operation.<sup>1</sup> Compared to the traditional redox-neutral processes that generally involve the performance of organometallic reagents as nucleophilic coupling partners,<sup>2</sup> nickel-catalysed reductive olefin DCF by harnessing two electrophiles across C=C bonds has attracted increasing attention as such an alternative strategy bypasses the use of sensitive organometallics and features mild conditions and broad functional group compatibility.<sup>3</sup> However, most of the reductive olefin DCFs rely on the coupling of two organohalide electrophiles, and thus, endeavouring to explore the reliability of other distinct and abundant electrophiles in olefin reductive DCF to broaden the structural and functional diversity of target molecules is highly desirable.

Aldehydes, in particular, are abundant and versatile building blocks in organic synthesis, while their application in catalytic reductive olefin DCF has been much less explored. An early

example is from the Montgomery group who reported Ni(cod)<sub>2</sub>-catalyzed three-component reaction of acrylates, aryl iodides and aldehydes under net reductive conditions with a stoichiometric amount of ZnMe<sub>2</sub> as the reductant (Scheme 1a).<sup>4</sup> Later on, Gall and co-workers reported a similar transformation on using CoBr<sub>2</sub> as the catalyst and Zn dust as the reductant.<sup>5</sup> These reductive processes provide a complementary approach to a classical



Scheme 1 Nickel-catalysed alkene dicarbofunctionalization with aldehydes as electrophiles.

<sup>a</sup>Key Laboratory of Material Chemistry for Energy Conversion and Storage, Ministry of Education, Hubei Key Laboratory of Bioinorganic Chemistry and Materia Medica, School of Chemistry and Chemical Engineering, Huazhong University of Science and Technology (HUST), 1037 Luoyu Road, Wuhan 430074, PR China. E-mail: yuanwm@hust.edu.cn

<sup>b</sup>Shenzhen Huazhong University of Science and Technology Research Institute, Shenzhen 518000, PR China

<sup>c</sup>Guangdong Provincial Key Laboratory of Catalysis, Southern University of Science and Technology, Shenzhen 518055, PR China

† Electronic supplementary information (ESI) available: Experimental procedures, characterization data, and copy of NMR spectra. CCDC 2217184, 2217195 and 2217198. For ESI and crystallographic data in CIF or other electronic format see DOI: <https://doi.org/10.1039/d2sc06303d>



conjugate addition/aldol tandem sequence<sup>6</sup> that requires sensitive arylmetallic reagents. However, the requirement of stoichiometric amounts of metal-based reductants inevitably produces a lot of metal salt waste and results in a certain degree of difficulty for synthetic scalability and practicability.

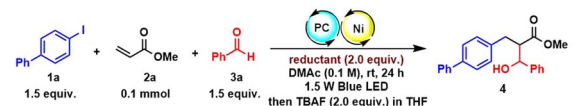
Taking advantage of the ability of the photoredox-assisted single-electron transfer (SET) process, researchers have recently applied Ni/photoredox dual catalysis<sup>7</sup> to the area of cross-electrophile coupling reactions,<sup>8</sup> enabling the coupling of organohalides in the absence of a stoichiometric metal reductant. However, most reported photo-redox-assisted reductive cross-couplings are limited to the two-component version<sup>9</sup> with few exceptions have been extended to the intermolecular three-component reaction of aryl and alkyl halides across alkenes.<sup>10</sup> Giving our longstanding interest in metallaphotoredox catalysis,<sup>9e,11</sup> we reported here a Ni/photoredox-catalysed three-component conjunctive cross-electrophile coupling of aryl halides with aldehydes and alkenes (Scheme 1b). We envisioned that the key to success of this tandem transformation is to identify a suitable organic reductant as any organic reductants release protons might be problematic because they can protonate each tentative C–Ni bond species, thus producing unwanted outcomes such as a dehalogenation product and reductive Heck product. As such, the most commonly used organic reductants in literature including tertiary amines and Hantzsch esters (HEs) would be inferior to the reaction because they can release protons when using as reductant. To address this issue, we envisioned that  $\alpha$ -silylamines might be a sort of valid organic reductant to furnish this tandem process as they release silylium ions instead of protons during the single electron oxidation stage. Moreover, the *in situ* generated silylium ion could act as a Lewis acid to activate aldehydes to promote the subsequent aldol reaction.  $\alpha$ -Silylamines have been widely used as  $\alpha$ -amino radical precursors in photocatalytic radical transformations,<sup>12</sup> while their potential as mild organic reductants in reductive cross-couplings has not yet been explored. Here, we disclose the unique functions of  $\alpha$ -silylamine in reductive conjugate addition/aldol tandem transformation.

## Results and discussion

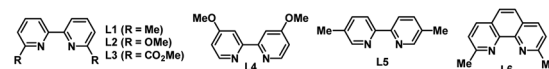
Our initial studies began with an investigation of various organic reductants. The three-component reductive conjugate addition/aldol tandem reaction with 4-iodo-1,1'-biphenyl (**1a**), methyl acrylate (**2a**), and benzaldehyde (**3a**) was performed in the presence of 1 mol% of Ir[dF(CF<sub>3</sub>)ppy]<sub>2</sub>(dtbbpy)PF<sub>6</sub>, 10 mol% of NiBr<sub>2</sub>·DME, and 10 mol% of 6,6'-di(Me)bpy in DMAc (0.1 M) at room temperature under 1.5 W blue LED irradiation for 24 h. Various organic reductants including Hantzsch ester (HE), Et<sub>3</sub>N, iPr<sub>2</sub>NEt, and *N,N,N',N'*-tetramethylethylenediamine (TMEDA) were examined with or without an extra base. Regrettably, all attempts failed to deliver any desired product. Instead, a huge amount of dehalogenation product **7** and/or reductive Heck product **5** was detected, suggesting that these proton-releasing organic reductants are not suitable for the transformation. Based on our previous work on nickel/photoredox-catalysed alkene dicarbofunctionalization,<sup>11a</sup> we tried to use an  $\alpha$ -silyl substituted tertiary amine such as 1-((trimethylsilyl)methyl)piperidine as the organic reductant due to its

easy preparation, low oxidation potential, and above all, because there are no protons released in the process. To our delight, the desired  $\beta$ -hydroxyl ester product **4** could be detected in 23% GC yield after the reaction with TBAF to remove the silyl group. Under this condition, only a trace amount of the dehalogenation product was detected. However, the reductive Heck product **5** and reductive carbonyl Heck product **6** were detected in 21% and 12% yield, respectively. After the initial result was obtained, we further examined other reaction parameters (Table 1). The screening of photocatalysts showed that Ir(ppy)<sub>3</sub> is the most efficient photocatalyst (entries 1–4). *Ortho*-substituted bipyridines are prevailing ligands and 6,6'-di(OMe)bpy is proven to be the best (entries 5–9). NiBr<sub>2</sub> and Ni(cod)<sub>2</sub> could also promote the reaction and give

Table 1 Condition optimization

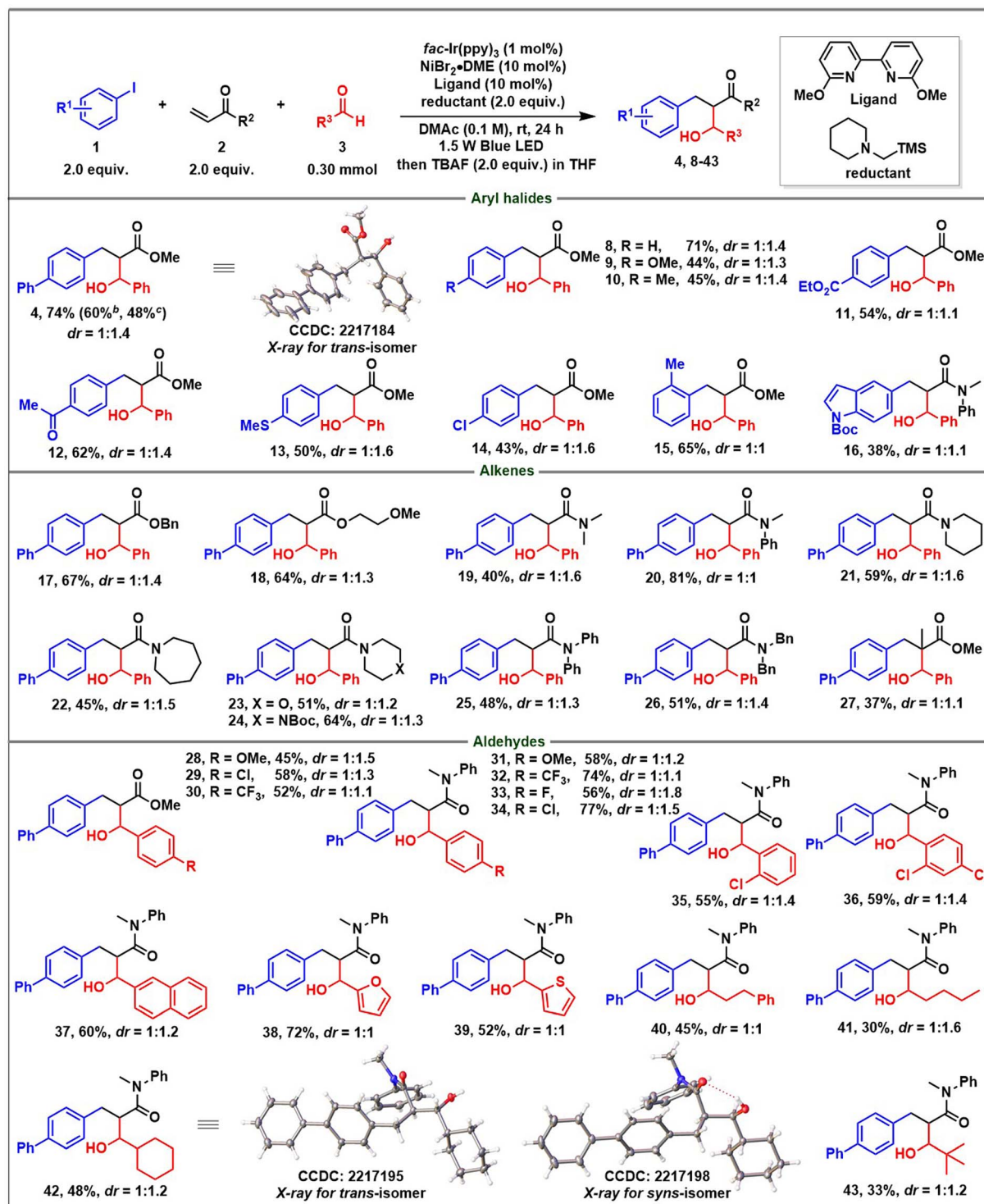


Entry <sup>b</sup>	Photocatalyst	[Ni]	Ligand	Solvent	4	5	6
1	Ir(ppy) <sub>3</sub>	NiBr <sub>2</sub> ·DME	L1	DMAc	34	23	21
2	Ir(ppy) <sub>2</sub> bpyPF <sub>6</sub>	NiBr <sub>2</sub> ·DME	L1	DMAc	21	11	43
3	Ru(bpy) <sub>3</sub> (PF <sub>6</sub> ) <sub>2</sub>	NiBr <sub>2</sub> ·DME	L1	DMAc	32	16	5
4	4-CzIPN	NiBr <sub>2</sub> ·DME	L1	DMAc	15	0	62
5	Ir(ppy) <sub>3</sub>	NiBr <sub>2</sub> ·DME	L2	DMAc	62	20	5
6	Ir(ppy) <sub>3</sub>	NiBr <sub>2</sub> ·DME	L3	DMAc	44	22	1
7	Ir(ppy) <sub>3</sub>	NiBr <sub>2</sub> ·DME	L4	DMAc	19	9	3
8	Ir(ppy) <sub>3</sub>	NiBr <sub>2</sub> ·DME	L5	DMAc	21	8	4
9	Ir(ppy) <sub>3</sub>	NiBr <sub>2</sub> ·DME	L6	DMAc	24	16	51
10	Ir(ppy) <sub>3</sub>	NiBr <sub>2</sub>	L2	DMAc	45	13	2
11	Ir(ppy) <sub>3</sub>	Ni(cod) <sub>2</sub>	L2	DMAc	55	4	10
12	Ir(ppy) <sub>3</sub>	NiBr <sub>2</sub> ·DME	L2	DMF	3	0	4
13	Ir(ppy) <sub>3</sub>	NiBr <sub>2</sub> ·DME	L2	MeCN	24	43	2
14	Ir(ppy) <sub>3</sub>	NiBr <sub>2</sub> ·DME	L2	THF	0	3	0
15 <sup>c</sup>	Ir(ppy) <sub>3</sub>	NiBr <sub>2</sub> ·DME	L2	DMAc	78	43	0
16	—	NiBr <sub>2</sub> ·DME	L2	DMAc	0	0	0
17 <sup>d</sup>	Ir(ppy) <sub>3</sub>	NiBr <sub>2</sub> ·DME	L2	DMAc	0	0	0
18	Ir(ppy) <sub>3</sub>	—	L2	DMAc	0	0	0
19	Ir(ppy) <sub>3</sub>	NiBr <sub>2</sub> ·DME	—	DMAc	44	13	0
20 <sup>e</sup>	Ir(ppy) <sub>3</sub>	NiBr <sub>2</sub> ·DME	L2	DMAc	22	4	50
21 <sup>f</sup>	Ir(ppy) <sub>3</sub>	NiBr <sub>2</sub> ·DME	L2	DMAc	15	6	8



<sup>a</sup> Ir[dF(CF<sub>3</sub>)ppy]<sub>2</sub>(dtbbpy)PF<sub>6</sub> (1 mol%), NiBr<sub>2</sub>·DME (10 mol%), and 6,6'-di(Me)bpy (10 mol%). Yields are determined by GC with *n*-tridecane as the internal standard. <sup>b</sup> Reaction conditions: photocatalyst (1 mol%), Ni catalyst (10 mol%), and ligand (10 mol%). <sup>c</sup> The molar ratio of **1a** : **2a** : **3a** = 2 : 2 : 1. <sup>d</sup> No light irradiation. <sup>e</sup> 4-Bromo-1,1'-biphenyl instead of **1a**. <sup>f</sup> [1,1'-biphenyl]-4-yl trifluoromethanesulfonate instead of **1a**.



Table 2 Substrate scope for nickel/photoredox dual-catalysed reductive conjugate addition/aldol tandem reaction<sup>a</sup>

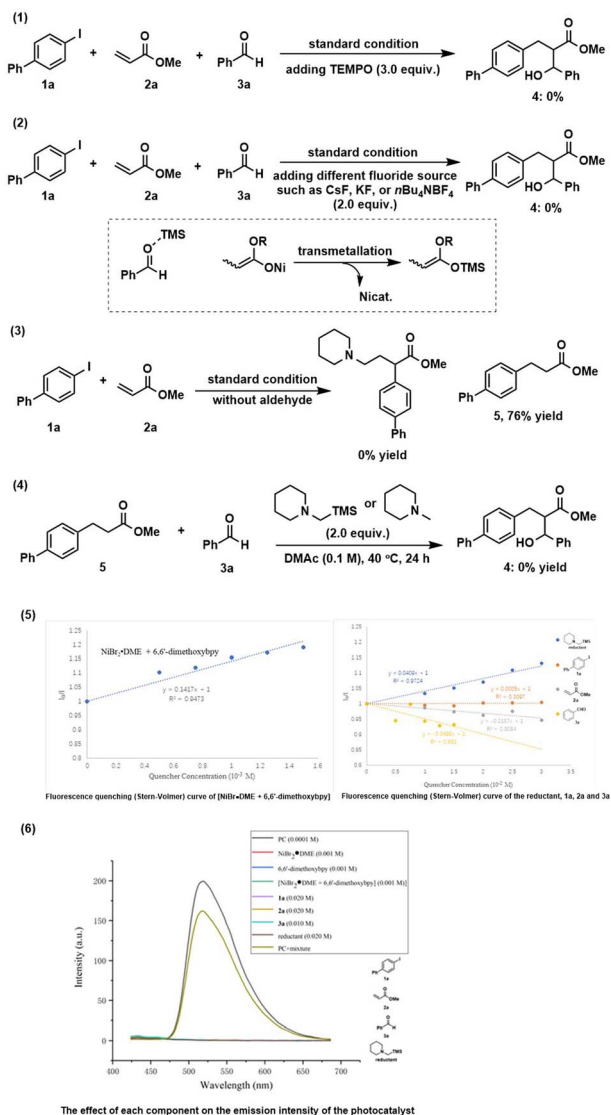
<sup>a</sup> All reactions were carried out on a 0.3 mmol scale under the optimized conditions (Table 1, entry 15). All yields are isolated yields. The diastereoselectivities were determined by crude <sup>1</sup>H NMR analysis. <sup>b</sup> 1 mmol scale. <sup>c</sup> 3 mmol scale.

a slightly lower yield (entries 10 and 11). The solvent has a dramatic influence on the reactivity (entries 12–14): DMF could only afford a trace amount of the product. Other less polar solvents

such as MeCN or THF were all inferior to the reaction, which either results in a large decrease in yield or completely retards the reaction. The mole ratio of each component also affects the reaction







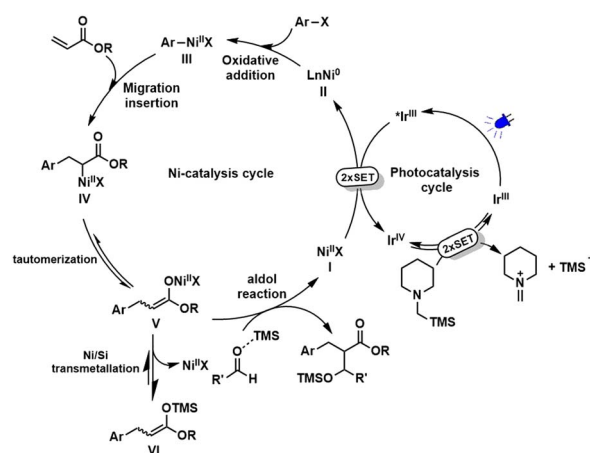
Scheme 2 Control experiments and spectroscopic investigations.

and the highest yield of 78% could be obtained when using benzaldehyde as the limiting reagent (entry 15). Under the optimized conditions, reductive carbonyl Heck product 6 and dehalogenation product 7 were successfully inhibited. Not surprisingly, the yield of reductive Heck product 5 was increased due to the addition of an excess amount of 1a and 2a. The control experiments revealed that the photocatalyst, nickel and visible light are indispensable (entries 16–18). Interestingly, omitting a ligand could still afford 44% yield of the desired product (entry 19). Replacing aryl iodide with aryl bromide or aryl triflate gives a largely decreased yield for the desired outcome (entries 20 and 21).

With the optimized reaction conditions in hand, we started to evaluate the scope generality of the three-component reaction (Table 2). First, a series of aryl iodides were examined. Aryl iodides with electron-donating and electron-withdrawing groups including phenyl (4), OMe (9), ester (11), ketone (12), SMe (13), and Cl (14)

were well tolerated, delivering the corresponding products in moderate to good yields. A sterically hindered substrate such as *ortho*-methyl substituted iodobenzene (15) also reacted with a good yield. Heteroaryl iodide was tolerated as well (16). The structure of the *trans*-configuration of product 4 was determined by X-ray diffraction analysis. Regarding the scope of alkenes, except for different substituted acrylates (4, 17, and 18), various *N*-substituted acrylamides were investigated. Acyclic acrylamides (19, 20, 25, and 26) and cyclic acrylamides (21–24) all reacted smoothly and afforded a series of structurally abundant  $\beta$ -hydroxyl amide products. Particularly,  $\alpha$ -methyl substituted methyl acrylate was also tolerated, enabling a product with an all-carbon quaternary stereocenter (27). Finally, the scope generality of aldehydes was evaluated. Again, not only electron-donating groups, but electron-withdrawing groups were also compatible (28–34). Sterically *ortho*-substituted benzaldehydes have no impact on the reactivity (35, 36). Of note, more reactive naphthaldehyde (37), furfural (38) and 2-thenaldehyde (39) successfully underwent conjugative coupling. Pleasingly, aliphatic aldehydes irrespective of containing an  $\alpha$ -primary, or secondary, or tertiary alkyl substituent were smoothly incorporated (40–43). Both structures of *trans*- and *syn*-configuration of product 42 were determined by X-ray diffraction analysis. Regrettably, the reaction could only give a poor stereocontrol with diastereoisomeric ratios ranging from 1 : 1 to 2 : 1. The low level of diastereoselectivity might have contributed to the poor selectivity of the formed *Z*- vs. *E*-enolate in the conjugate addition step or the absence of a Zimmerman–Traxler-type transition state in the second aldol reaction step.<sup>13</sup> We also added some metal-based Lewis acids such as  $\text{ZnCl}_2$  and  $\text{MgCl}_2$  to improve diastereoselection, but no further improvement was obtained. Anyway, both diastereoisomers can be separated by column chromatography on silica gel. The reaction could be scaled-up to 1 mmol (60%) and 3 mmol (48%) with an acceptable yield obtained.

In order to gain insight into the reaction mechanism, some control experiments were conducted. The reaction was completely inhibited by adding radical scavenger TEMPO [(2,2,6,6-tetramethylpiperidin-1-yl)oxyl] (Scheme 2(1)). Besides, all reactions failed to deliver any desired product when various different fluoride sources added (Scheme 2(2)). We speculated



Scheme 3 Proposed mechanism.

that the *in situ* generated silylium ion species (see the mechanistic discussion) was trapped by a fluoride source to form the useless TMSF. These interesting results indicate the significant importance of silyl groups for this reaction. We deduced that the TMS group plays at least two roles: (1) may serve as a Lewis acid to activate a carbonyl group for aldol reaction; (2) regenerate the active nickel catalyst *via* transmetallation of the O–Ni bond to the stronger O–Si bond. A control experiment without aldehyde was performed where no three-component conjunctive addition product was detected, and only a large amount of reductive Heck product **5** was afforded (Scheme 2(3)), suggesting that an  $\alpha$ -amino radical might not be generated<sup>11a</sup> under this condition. The intermediate **5** may possibly react with aldehyde in the presence of a base under thermal conditions to get the final product. However, the reaction cannot produce **4**, thus excluding this possibility (Scheme 2(4)). To better understand the behavior of the photoexcited step, Stern–Volmer fluorescence quenching experiments<sup>14</sup> were performed (see the ESI† for details). The results revealed that the oxidative quenching of the excited state of the photocatalyst by the nickel(II) catalyst is much more efficient over other components (Scheme 2(5)), suggesting that a single-electron-transfer (SET) event occurred between the nickel(II) catalyst and \*Ir(ppy)<sub>3</sub> that initiates the photocatalytic process. To exclude the possibility of the nickel complex affecting the emission intensity of the photocatalyst, the absorption spectra of each component were recorded and the results showed that all components have no absorption in this region (Scheme 2(6)).

Based on the above mechanistic studies and our previous reports,<sup>11</sup> a plausible mechanism was proposed for this reductive conjugate addition/aldol tandem sequence (Scheme 3). First, successive SET process between the photoexcited \*Ir<sup>III</sup> ( $E_{1/2}^{IV/III} = -1.73$  V *vs.* SCE)<sup>15</sup> and Ni<sup>II</sup> [ $E_{1/2}(\text{Ni}^{II}/\text{Ni}^0) = -1.2$  V *vs.* SCE]<sup>16</sup> generates Ni<sup>0</sup> and Ir<sup>IV</sup>. Ir<sup>IV</sup> possessing a strong reductive potential ( $E_{1/2}^{IV/III} = +0.77$  V *vs.* SCE)<sup>15</sup> can oxidize  $\alpha$ -silylamine ( $E_{1/2}^{\text{ox}} = +0.71$  V *vs.* SCE)<sup>17,18</sup> to get iminium ion by successive SET. Meanwhile, Ir<sup>IV</sup> is reduced back to the ground state of Ir<sup>III</sup>. On the other hand, Ni<sup>0</sup> species undergoes oxidative addition with ArX to afford ArNi<sup>II</sup>X, followed by migration insertion into C=C bond to get  $\alpha$ -carbonyl-Ni<sup>II</sup> intermediate (**IV**). An equilibration between nickel *O*-enolate (**V**) and *C*-enolate (**IV**) tautomer is possible,<sup>19</sup> which could be further transformed into a more stable silyl ketene acetal (**VI**) *via* a Ni/Si transmetallation. Final aldol reaction promoted by Lewis acidic silylium ion delivers products and regenerate Ni<sup>II</sup> catalyst.

## Conclusions

In summary, we report here a nickel/photoredox dual catalytic platform for enabling a reductive conjugate addition/aldol reaction with aryl halides, electron-deficient alkenes, and aldehydes.  $\alpha$ -Silylamine is identified as an efficient organic reductant due to its unique properties. Our strategy provides a complementary route to previous procedures that bypassing the use of organometallic reagents or metal reductants for this three-component transformation. Further studies on designing asymmetric reaction and gaining a deep insight into the mechanism are currently ongoing in the laboratory.

## Data availability

All experimental and characterization data, as well as NMR spectra are available in the ESI.† Crystallographic data for compound **4** and **42** have been deposited in the Cambridge Crystallographic Data Centre under accession number CCDC 2217184, 2217195, and 2217198.

## Author contributions

H. Z. performed all the experiments and prepared the ESI.† W. Y. supervised the research and wrote the manuscript.

## Conflicts of interest

The authors declare no competing financial interest.

## Acknowledgements

We are grateful to the National Natural Science Foundation of China (22201087), Guangdong Basic and Applied Basic Research Foundation (2019A1515110788, 2022A1515012507), Guangdong Provincial Key Laboratory of Catalysis (2020B121201002), and the Innovation and Talent Recruitment Base of New Energy Chemistry and Device (B21003) of Huazhong University of Science and Technology (HUST) for the financial support.

## Notes and references

- For selected reviews on transition-metal-catalysed 1,2-dicarbofunctionalization of alkenes, see: (a) R. K. Dhungana, S. Kc, P. Basnet and R. Giri, *Chem. Rev.*, 2018, **18**, 1314; (b) J. Derosa, O. Apolinar, T. Kang, V. T. Tran and K. M. Engle, *Chem. Sci.*, 2020, **11**, 4287; (c) X. Qi and T. Diao, *ACS Catal.*, 2020, **10**, 8542; (d) S. Zhu, X. Zhao, H. Li and L. Chu, *Chem. Soc. Rev.*, 2021, **50**, 10836.
- For selected examples of nickel-catalysed 1,2-dicarbofunctionalization of alkenes involving organometallics, see: (a) J. Derosa, V. T. Tran, M. N. Boulous, J. S. Chen and K. M. Engle, *J. Am. Chem. Soc.*, 2017, **139**, 10657; (b) B. Shrestha, P. Basnet, R. K. Dhungana, S. Kc, S. Thapa, J. M. Sears and R. Giri, *J. Am. Chem. Soc.*, 2017, **139**, 10653; (c) M. Chierchia, P. Xu, G. J. Lovinger and J. P. Morken, *Angew. Chem., Int. Ed.*, 2019, **58**, 14245; (d) W. Li, J. K. Boon and Y. Zhao, *Chem. Sci.*, 2018, **9**, 600; (e) T. Qin, J. Cornella, C. Li, L. R. Malins, J. T. Edwards, S. Kawamura, B. D. Maxwell, M. D. Eastgate and P. S. Baran, *Science*, 2016, **352**, 801; (f) J.-W. Gu, Q.-Q. Min, L.-C. Yu and X. Zhang, *Angew. Chem., Int. Ed.*, 2016, **55**, 12270; (g) P. Gao, L.-A. Chen and M. K. Brown, *J. Am. Chem. Soc.*, 2018, **140**, 10653; (h) H. Wang, C.-F. Liu, R. T. Martin, O. Gutierrez and M. J. Koh, *Nat. Chem.*, 2022, **14**, 188; (i) O. Apolinar, T. Kang, T. M. Alturafi, P. G. Bedekar, C. Z. Rubel, J. Derosa, B. B. Sanchez, Q. N. Wong, E. J. Sturgell, J. S. Chen, S. R. Wisniewski, P. Liu and K. M. Engle, *J. Am. Chem. Soc.*, 2022, **144**, 19337;



- (j) C.-F. Liu, Z.-C. Wang, X. Luo, J. Lu, C. H. M. Ko, S.-L. Shi and M. J. Koh, *Nat. Catal.*, 2022, **5**, 934.
- 3 For recent progress of Ni-catalysed reductive conjunctive cross-coupling of alkenes, see: (a) A. García-Domínguez, Z. Li and C. Nevado, *J. Am. Chem. Soc.*, 2017, **139**, 6835; (b) W. Shu, A. García-Domínguez, M. T. Quirós, R. Mondal, D. J. Cárdenas and C. Nevado, *J. Am. Chem. Soc.*, 2019, **141**, 13812; (c) H.-Y. Tu, F. Wang, L. Huo, Y. Li, S. Zhu, X. Zhao, H. Li, F.-L. Qing and L. Chu, *J. Am. Chem. Soc.*, 2020, **142**, 9604; (d) D. Anthony, Q. Lin, J. Baudet and T. Diao, *Angew. Chem., Int. Ed.*, 2019, **58**, 3198; (e) X.-X. Wang, X. Lu, S.-J. He and Y. Fu, *Chem. Sci.*, 2020, **11**, 7950; (f) T. Yang, Y. Jiang, Y. Luo, J. J. H. Lim, Y. Lan and M. J. Koh, *J. Am. Chem. Soc.*, 2020, **142**, 21410; (g) X. Xi, Y. Chen and W. Yuan, *Org. Lett.*, 2022, **24**, 3938; (h) J.-X. Zhang and W. Shu, *Org. Lett.*, 2022, **24**, 3844; (i) T. Yang, X. Chen, W. Rao and M. J. Koh, *Chem*, 2020, **6**, 738.
- 4 K. Subburaj and J. Montgomery, *J. Am. Chem. Soc.*, 2003, **125**, 11210.
- 5 J. Paul, M. Presset, F. Cantagrel, E. L. Gall and E. Léonel, *Chem.-Eur. J.*, 2017, **23**, 402.
- 6 For selected reviews, see: (a) H.-C. Guo and J.-A. Ma, *Angew. Chem., Int. Ed.*, 2006, **45**, 354; (b) T. Jerphagnon, M. G. Pizzuti, A. J. Minnaard and B. L. Feringa, *Chem. Soc. Rev.*, 2009, **38**, 1039.
- 7 For selected reviews on TM/photoredox catalysis, see: (a) K. L. Skubi, T. R. Blum and T. P. Yoon, *Chem. Rev.*, 2016, **116**, 10035; (b) J. C. Tellis, C. B. Kelly, D. N. Primer, M. Jouffroy, N. R. Patel and G. A. Molander, *Acc. Chem. Res.*, 2016, **49**, 1429; (c) A. Y. Chan, I. B. Perry, N. B. Bissonnette, B. F. Buksh, G. A. Edwards, L. I. Frye, O. L. Garry, M. N. Lavagnino, B. X. Li, Y. Liang, E. Mao, A. Millet, J. V. Oakley, N. L. Reed, H. A. Sakai, C. P. Seath and D. W. C. MacMillan, *Chem. Rev.*, 2022, **122**, 1485.
- 8 For selected reviews, see: (a) D. J. Weix, *Acc. Chem. Res.*, 2015, **48**, 1767; (b) J. Gu, X. Wang, W. Xue and H. Gong, *Org. Chem. Front.*, 2015, **2**, 1411.
- 9 For recent reports on cross-electrophile reactions under Ni-photoredox catalysis, see: (a) Z. Duan, W. Li and A. Lei, *Org. Lett.*, 2016, **18**, 4012; (b) P. Zhang, C. C. Le and D. W. C. MacMillan, *J. Am. Chem. Soc.*, 2016, **138**, 8084; (c) J. Yi, S. O. Badir, L. M. Kammer, M. Ribagorda and G. A. Molander, *Org. Lett.*, 2019, **21**, 3346; (d) M. Parasram, B. J. Shields, O. Ahmad, T. Knauber and A. G. Doyle, *ACS Catal.*, 2020, **10**, 5821; (e) X. Xi, Y. Luo, W. Li, M. Xu, H. Zhao, Y. Chen, S. Zheng, X. Qi and W. Yuan, *Angew. Chem., Int. Ed.*, 2022, e202114731; (f) H. Guan, Q. Zhang, P. J. Walsh and J. Mao, *Angew. Chem., Int. Ed.*, 2020, **59**, 5172.
- 10 (a) S.-Z. Sun, Y. Duan, R. S. Mega, R. J. Somerville and R. Martin, *Angew. Chem., Int. Ed.*, 2020, **59**, 4370; (b) P. Qian, H. Guan, Y.-E. Wang, Q. Lu, F. Zhang, D. Xiong, P. J. Walsh and J. Mao, *Nat. Commun.*, 2021, **12**, 6613; (c) A. Luridiana, D. Mazzarella, L. Capaldo, J. A. Rincón, P. García-Losada, C. Mateos, M. O. Frederick, M. Nuño, W. J. Buma and T. Noël, *ACS Catal.*, 2022, **12**, 11216.
- 11 (a) S. Zheng, Z. Chen, Y. Hu, X. Xi, Z. Liao, W. Li and W. Yuan, *Angew. Chem., Int. Ed.*, 2020, **59**, 17910; (b) S. Zheng, W. Wang and W. Yuan, *J. Am. Chem. Soc.*, 2022, **144**, 17776.
- 12 K. Nakajima, Y. Miyake and Y. Nishibayashi, *Acc. Chem. Res.*, 2016, **49**, 1946.
- 13 H. E. Zimmerman and M. D. Traxler, *J. Am. Chem. Soc.*, 1957, **79**, 1920.
- 14 N. J. Turro, *Modern Molecular Photochemistry*, Benjamin/Cummings, Menlo Park, CA, 1978.
- 15 C. K. Prier, D. A. Rankic and D. W. C. MacMillan, *Chem. Rev.*, 2013, **113**, 5322.
- 16 Z. Zuo, D. T. Ahneman, L. Chu, J. A. Terrett, A. G. Doyle and D. W. C. MacMillan, *Science*, 2014, **345**, 437.
- 17 C. Remeur, C. B. Kelly, N. R. Patel and G. A. Molander, *ACS Catal.*, 2017, **7**, 6065.
- 18 Given the fact that  $\alpha$ -amino radical ( $E_{1/2}^{\text{ox}} \approx -1.0$  V vs. SCE) is more readily oxidized than the starting material  $\alpha$ -silylamine ( $E_{1/2}^{\text{ox}} = +0.4-0.8$  V vs. SCE), it can undergo a successive single-electron oxidation process to get iminium ion species and release silylium ions. For data of the redox-potentials, see: (a) J. Yoshida, T. Maekawa, T. Murata, S. Matsunaga and S. Isoe, *J. Am. Chem. Soc.*, 1990, **112**, 1962; (b) D. D. M. Wayner, J. J. Dannenberg and D. Griller, *Chem. Phys. Lett.*, 1986, **131**, 189.
- 19 (a) J. Cámpora, C. M. Maya, P. Palma, E. Carmona, E. Gutiérrez, C. Ruiz, C. Graiff and A. Tiripicchio, *Chem.-Eur. J.*, 2005, **11**, 6889; (b) E. R. Burkhardt, R. G. Bergman and C. H. Heathcock, *Organometallics*, 1990, **9**, 30.

